

## Surface Chemistry

Deutsche Ausgabe: DOI: 10.1002/ange.201602572  
Internationale Ausgabe: DOI: 10.1002/anie.201602572

## Constitutional Dynamics of Metal–Organic Motifs on a Au(111) Surface

Huihui Kong, Chi Zhang, Lei Xie, Likun Wang, and Wei Xu\*

**Abstract:** Constitutional dynamic chemistry (CDC), including both dynamic covalent chemistry and dynamic noncovalent chemistry, relies on reversible formation and breakage of bonds to achieve continuous changes in constitution by reorganization of components. In this regard, CDC is considered to be an efficient and appealing strategy for selective fabrication of surface nanostructures by virtue of dynamic diversity. Although constitutional dynamics of monolayered structures has been recently demonstrated at liquid/solid interfaces, most of molecular reorganization/reaction processes were thought to be irreversible under ultrahigh vacuum (UHV) conditions where CDC is therefore a challenge to be achieved. Here, we have successfully constructed a system that presents constitutional dynamics on a solid surface based on dynamic coordination chemistry, in which selective formation of metal–organic motifs is achieved under UHV conditions. The key to making this reversible switching successful is the molecule–substrate interaction as revealed by DFT calculations.

Supramolecular chemistry, which is intrinsically a dynamic chemistry, has been widely employed as an efficient way to construct highly complex and multifunctional nanostructures through self-assembly processes from rationally designed molecular building blocks.<sup>[1,2]</sup> As one of the novel types of dynamic processes, constitutional dynamics, which relies on reversible formation and breakage of bonds to achieve continuous changes in constitution by reorganization of components, has recently been considered to be an appealing strategy for controllable fabrication of surface nanostructures with selection in addition to design.<sup>[3,4]</sup> In this regard, as an important outgrowth of supramolecular chemistry, constitutional dynamic chemistry would be promising for potential applications in molecular switching devices. Recently, constitutional dynamics of monolayered structures (including both covalent bonds and noncovalent interactions) has been demonstrated at liquid/solid interfaces.<sup>[5–10]</sup> However, most of molecular reorganization/reaction processes investigated under ultrahigh vacuum (UHV) conditions were thought to be irreversible,<sup>[11–15]</sup> and constitutional dynamics is therefore a challenge to be achieved under UHV conditions. Recently, chirality switching of caged supramolecules was observed as

an evidence of constitutional dynamics under UHV conditions, while the process was in a stochastic manner without control on the dynamers.<sup>[16]</sup> It is therefore of utmost interest to develop systems that present self-organization with selection operating on constitutional diversity under UHV conditions.

In this study, we choose a nucleobase molecule, thymine (T), as a potential candidate to interact with Ni atoms. As the T molecule contains two possible coordination binding sites (i.e. O2 and O4, see the upper panel of Figure 1), from theoretical calculations, both sites are capable of coordinating to Ni atoms with similar stabilities. It thus may provide us with

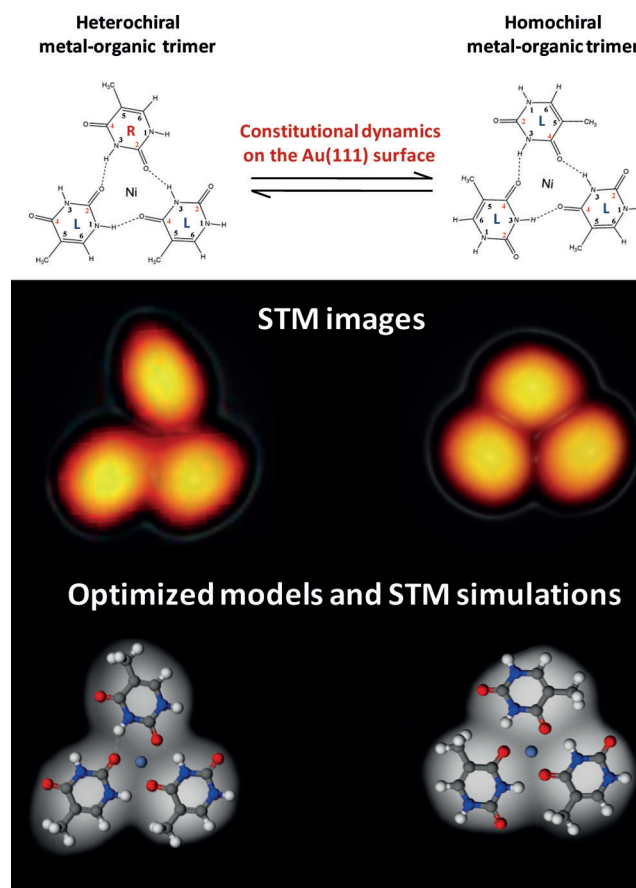


**Figure 1.** Upper panel: Schematic illustration on the constitutional dynamics between two distinct metal–organic coordination trimers on a Au(111) surface. R and L denote the chiralities of individual molecules. Lower panel: Close-up STM images and corresponding STM simulations superimposed with optimized models of heterochiral and homochiral metal–organic trimers on Au(111). Scanning conditions:  $I_t = 0.78$  nA,  $V_t = 1.25$  V; STM simulations are performed at a bias voltage of 1.2 V.

[\*] H. H. Kong, C. Zhang, L. Xie, L. Wang, Prof. Dr. W. Xu  
Tongji-Aarhus Joint Research Center for Nanostructures and  
Functional Nanomaterials, College of Materials Science and  
Engineering, Tongji University, Caoan Road 4800, Shanghai 201804  
(P.R. China)  
E-mail: xuwei@tongji.edu.cn

Supporting information for this article can be found under:  
<http://dx.doi.org/10.1002/anie.201602572>.

a model system presenting structural diversity to allow investigation of dynamic coordination chemistry related issues on the surface. Herein, from the interplay of high-resolution STM imaging and density functional theory (DFT) calculations, we have realized continuous interconversions of two distinct metal–organic trimers on the Au(111) surface (see Figure 1), thus achieved on-surface constitutional dynamics under UHV conditions, in which these two metal–organic motifs just behave as dynamers (i.e. supramolecules that are able to undergo adaptation and continuous constitutional changes). The key to making this controllable switching successful is the molecule–substrate interaction, that is, the preferred registry of metal–organic trimers with respect to the surface atomic lattice, which is revealed by extensive DFT calculations.

Co-deposition of T molecules and Ni atoms on a Au(111) surface held at room temperature (RT) leads to the formation of one-dimensional (1D) molecular chains as shown in Figure 2a. These chains look similar to hydrogen-bonded T filaments (see Figure S1) at a first glance, however, they

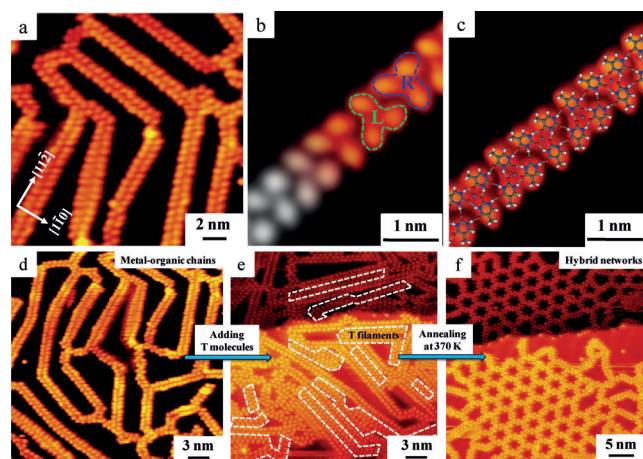


**Figure 2.** a) Large-scale STM image showing the formation of metal–organic molecular chains after co-deposition of T molecules and Ni atoms on the surface held at RT. b) Close-up STM image allowing us to identify the individual building blocks (i.e. heterochiral metal–organic trimers indicated by green and blue contours where R and L denote the chiralities of the motifs) within the chain structure. The STM simulation (the gray part) is partially superimposed on the STM image. c) DFT-optimized structural model superimposed on the STM image. d–f) Structural conversion from metal–organic chains to hybrid networks by adding additional T molecules and then annealing at 370 K. The newly added T molecules are indicated by white contours as shown in (e). Scanning conditions:  $I_t = 0.39$  nA,  $V_t = 1.25$  V; STM simulation is performed at a bias voltage of 1.25 V.

prefer to be separated even at a higher surface coverage (ca. 0.8 monolayer). This characteristic is different from hydrogen-bonded T filaments that are inclined to form 2D islands as shown in Figure S1.<sup>[17]</sup> From the close-up STM image (Figure 2b), we could identify that the molecular chain is composed of trimeric motifs with alternating chiralities as indicated by green and blue contours. This elementary structural motif is assigned to a heterochiral metal–organic trimer as highlighted in Figure 1. From the DFT-optimized

model and the STM simulation, we distinguish that it is formed by three T molecules (with different chiralities) coordinating to one Ni atom by O2 or O4 sites (also see the upper panel of Figure 1), and then each trimer binds to the neighboring one with opposite chirality through three N–H...O hydrogen bonds forming the metal–organic molecular chains as revealed by the optimized model overlaid on the STM image (Figure 2c). Such metal–organic chains are found to be similar to the 1D chains formed by glutamic acid and nickel atoms on Au(111), in which the growth directions of the chains are influenced by the herringbone reconstruction.<sup>[18]</sup> While, in our case, we can identify that basically there are three distinct growth directions and there is no obvious tendency that the directions and separations of the chains are influenced by the herringbone reconstruction as shown in Figures S2 and S3. If additional T molecules are deposited on the metal–organic chain-covered surface, we find the coexistence of metal–organic chains and hydrogen-bonded T filaments (Figure 2e). After annealing at 370 K, surprisingly, we find that the metal–organic chains are converted to a network structure (Figure 2f). Since it is not feasible to fabricate the network structure by direct anneal of the metal–organic chains at 370 K, we speculate that the newly added T molecules somehow facilitate the formation of the network structure.

From the close-up high-resolution STM image of the network structure (Figure 3a), we identify that the structure is composed of both trimeric and dimeric elementary motifs as indicated by green and blue contours, respectively (Figure 3b). The trimeric motif is assigned to a homochiral metal–organic trimer as highlighted in Figure 1. From the DFT-optimized model and the STM simulation, we distinguish that the homochiral trimer is formed by three T molecules (with

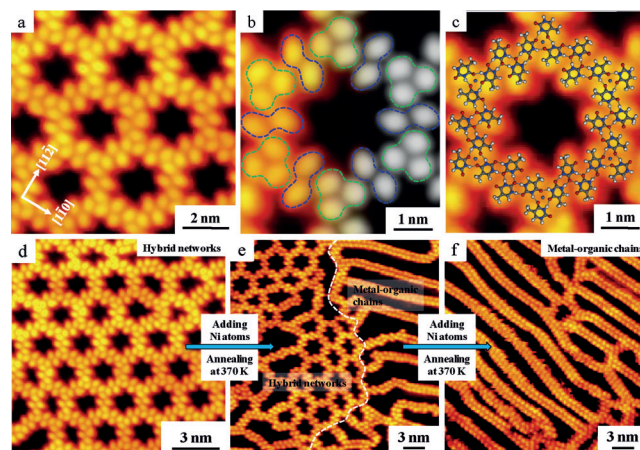


**Figure 3.** a) and b) Close-up high-resolution STM images of hybrid molecular networks allowing us to identify the individual building blocks (i.e. homochiral metal–organic trimers and hydrogen-bonded T dimers indicated by green and blue contours, respectively) within the network structure. The STM simulation (the gray part) is partially superimposed on the STM image. c) DFT-optimized structural model superimposed on the STM image. d–f) Reversible structural conversion from hybrid networks back to metal–organic chains by adding Ni atoms and then annealing at 370 K. Scanning conditions:  $I_t = 0.86$  nA,  $V_t = 1.25$  V; STM simulation is performed at a bias voltage of 1.25 V.



the same chirality) coordinating to one Ni atom by O4 sites (also see the upper panel of Figure 1), and the dimeric motif is assigned to a hydrogen-bonded T dimer (as shown in detail in Figure S4). The hybrid network structure is then formed by alternating arrangement of homochiral metal–organic trimers and hydrogen-bonded T dimers linked together through two N–H...O hydrogen bonds as revealed by the optimized model which is overlaid on the STM image (Figure 3c). Such hybrid network structures look similar to the previously reported porous networks formed by the adsorption of (*S*)-proline on Ni/Au(111).<sup>[19]</sup> The remarkable difference is that the hybrid network is formed by two kinds of elementary structural motifs as shown in Figure 3a–c. It is noteworthy that the introduction of additional T molecules does not change the local stoichiometric ratio for the metal–organic motifs (i.e., T/Ni ratio is kept as 3:1 in the homochiral metal–organic trimer). Thus, the hydrogen-bonded T dimers just facilitate the formation of the hybrid network structure.

To explore the role of additional T molecules in facilitating the conversion from the heterochiral metal–organic trimer to the homochiral one, an interesting question arises what happens if we remove the hydrogen-bonded T dimers. To do so, we sequentially deposit additional Ni atoms on the hybrid-networks-covered surface with an attempt to consume the hydrogen-bonded T dimers. After annealing such a surface at 370 K, interestingly, we find the hybrid networks are converted back to metal–organic chains (Figure 3d–f), which indicates that the reversible conversion from homochiral metal–organic trimers to heterochiral ones is also feasible. Furthermore, the continuous interconversions between two distinct metal–organic trimers have also been achieved as shown in the Supporting Information (Figure S5). In this system, these two metal–organic trimers just behave as dynamers that are able to undergo continuous constitutional changes. Consequently, we present a model system of on-surface constitutional dynamics based on dynamic coordination chemistry.

Finally, to unravel the mechanism of this unprecedented selective self-organization of metal–organic motifs, extensive DFT calculations are performed to discover the role of hydrogen-bonded T dimers in such a process. As known that for on-surface metal–organic motifs the molecule–substrate interaction (i.e. the preferred registry with respect to the substrate lattice) predominantly determines the stabilities of motifs,<sup>[20,21]</sup> we thus start out the calculations on the isolated heterochiral and homochiral metal–organic trimers adsorbed on Au(111). The most stable configurations for these two motifs are shown in Figure 4a,c, respectively. From the optimized models, we can see that for both heterochiral and homochiral trimers, the Ni atoms and the coordination O atoms are both located at hollow sites of the substrate lattices. The most stable heterochiral trimer is calculated to be slightly less stable than the homochiral one by 0.09 eV. Then the question arises why the formed surface structure is dominated by metal–organic chains (i.e. heterochiral trimers) before introducing additional T dimers on the surface.

We then calculate larger structures by directly linking two heterochiral trimers and two homochiral ones through hydrogen bonds as shown in Figure 4b,f, respectively. Again, from

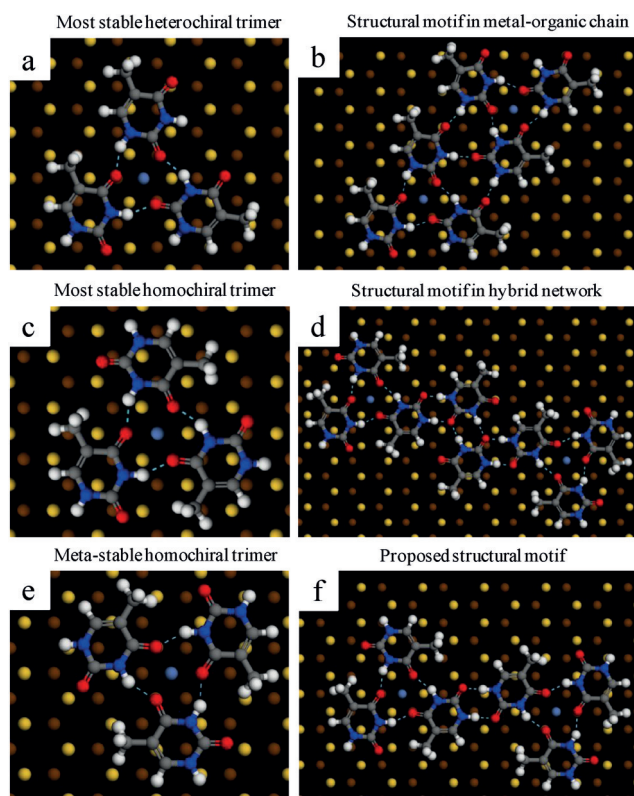


**Figure 4.** DFT-optimized models of heterochiral and homochiral metal–organic trimers and the corresponding larger structural motifs on a Au(111) surface. a) DFT-optimized models of the most stable isolated heterochiral metal–organic trimer, and b) two most stable heterochiral trimers directly linked by hydrogen bonds. c) DFT-optimized models of the most stable isolated homochiral metal–organic trimer, and d) two most stable homochiral trimers linked by a hydrogen-bonded T dimer through hydrogen bonds. e) DFT-optimized models of the metastable isolated homochiral metal–organic trimer, and f) one most stable and one *meta*-stable homochiral trimers directly linked by hydrogen bonds. The gold atoms in the first layer and second one are shown in yellow and brown, respectively.

the optimized model shown in Figure 4b which is just the structural motif in metal–organic chains, we distinguish that both heterochiral trimers adopt the most stable configuration. While, for the proposed structure shown in Figure 4f, we note that only one of the homochiral trimers adopts the most stable configuration, and the other one has to adopt a metastable configuration (Figure 4e) where the coordination O atoms are located at top sites of the substrate lattices. Thus, the structural motif formed by directly linking of two heterochiral trimers (Figure 4b) is energetically more favorable than that of two homochiral trimers (Figure 4f) by 0.27 eV, which well accounts for the formation of metal–organic chains composed of heterochiral trimers (Figure 2a–c). Furthermore, to dig out the role of T dimers in stabilizing the homochiral trimers, we calculate an even larger structure by incorporation of a hydrogen-bonded T dimer in between two homochiral trimers through hydrogen bonds as shown in Figure 4d. From the optimized model, which is just the structural motif in hybrid networks, we identify that both homochiral trimers now adopt the most stable configuration. In other words, the homochiral

metal–organic trimers are trapped by the hydrogen-bonded T dimers as experimentally evidenced (Figure 3 a–c).

In conclusion, from the interplay of high-resolution STM imaging and detailed DFT calculations, we have not only realized on-surface constitutional dynamics but also achieved the control on different dynamers, which was thought to be a challenge under UHV conditions. In this system, the key to making the constitutional dynamics successful is the molecule–substrate interaction, which affects the relative stabilities of different dynamers and thus leads to self-organization with selection. These findings may open a new avenue to controllable fabrication of nanostructures with variation and selection in a comparatively facile manner by making use of the strategy of surface-assisted dynamic chemistry, thus enabling adaptive chemistry on the surface.

### Acknowledgements

The authors acknowledge financial support from the National Natural Science Foundation of China (grant number 21473123), the Research Fund for the Doctoral Program of Higher Education of China (grant number 20120072110045).

**Keywords:** density functional theory · dynamic coordination chemistry · metal–organic motifs · scanning tunneling microscopy · surface chemistry

**How to cite:** *Angew. Chem. Int. Ed.* **2016**, *55*, 7157–7160  
*Angew. Chem.* **2016**, *128*, 7273–7276

- [1] J.-M. Lehn, *Supramolecular Chemistry: Concepts and Perspectives*, Wiley, Hoboken, **1995**.
- [2] J.-M. Lehn, *Angew. Chem. Int. Ed. Engl.* **1990**, *29*, 1304–1319; *Angew. Chem.* **1990**, *102*, 1347–1362.
- [3] J.-M. Lehn, *Chem. Soc. Rev.* **2007**, *36*, 151–160.
- [4] J.-M. Lehn, *Science* **2002**, *295*, 2400–2403.
- [5] A. Ciesielski, M. El Gharah, S. Haar, P. Kovaricek, J.-M. Lehn, P. Samori, *Nat. Chem.* **2014**, *6*, 1017–1023.
- [6] A. Ciesielski, S. Lena, S. Masiero, G. P. Spada, P. Samori, *Angew. Chem. Int. Ed.* **2010**, *49*, 1963–1966; *Angew. Chem.* **2010**, *122*, 2007–2010.
- [7] Y. H. Jin, C. Yu, R. J. Denman, W. Zhang, *Chem. Soc. Rev.* **2013**, *42*, 6634–6654.
- [8] A. Ciesielski, P. Samori, *Nanoscale* **2011**, *3*, 1397–1410.
- [9] S. L. Lee, Y. Fang, G. Velpula, F. R. Cometto, M. Lingenfelder, K. Mullen, K. S. Mali, S. De Feyter, *ACS Nano* **2015**, *9*, 11608–11617.
- [10] J. Plas, D. Waghay, J. Adisojojoso, O. Ivasenko, W. Dehaen, S. De Feyter, *Chem. Commun.* **2015**, *51*, 16338–16341.
- [11] H. H. Kong, Q. Sun, L. K. Wang, Q. G. Tan, C. Zhang, K. Sheng, W. Xu, *ACS Nano* **2014**, *8*, 1804–1808.
- [12] C. Zhang, L. Xie, L. K. Wang, H. H. Kong, Q. G. Tan, W. Xu, *J. Am. Chem. Soc.* **2015**, *137*, 11795–11800.
- [13] J. I. Urgel, D. Eciija, W. Auwarter, D. Stassen, D. Bonifazi, J. V. Barth, *Angew. Chem. Int. Ed.* **2015**, *54*, 6163–6167; *Angew. Chem.* **2015**, *127*, 6261–6265.
- [14] S. Weigelt, C. Busse, C. Bombis, M. M. Knudsen, K. V. Gothelf, T. Strunskus, C. Wöll, M. Dahlbom, B. Hammer, E. Laegsgaard, F. Besenbacher, T. R. Linderoth, *Angew. Chem. Int. Ed.* **2007**, *46*, 9227–9230; *Angew. Chem.* **2007**, *119*, 9387–9390.
- [15] S. Weigelt, C. Busse, C. Bombis, M. M. Knudsen, K. V. Gothelf, E. Laegsgaard, F. Besenbacher, T. R. Linderoth, *Angew. Chem. Int. Ed.* **2008**, *47*, 4406–4410; *Angew. Chem.* **2008**, *120*, 4478–4482.
- [16] D. Kuhne, F. Klappenberger, W. Krenner, S. Klyatskaya, M. Ruben, J. V. Barth, *Proc. Natl. Acad. Sci. USA* **2010**, *107*, 21332–21336.
- [17] W. Xu, R. E. A. Kelly, R. Otero, M. Schöck, E. Laegsgaard, I. Stensgaard, L. N. Kantorovich, F. Besenbacher, *Small* **2007**, *3*, 2011–2014.
- [18] A. G. Trant, T. E. Jones, C. J. Baddeley, *J. Phys. Chem. C* **2007**, *111*, 10534–10540.
- [19] R. T. Seljamäe-Green, G. J. Simpson, F. Grillo, J. Greenwood, S. M. Francis, R. Schaub, J. E. Gano, H. A. Fruchtl, P. Lacovig, C. J. Baddeley, *Langmuir* **2015**, *31*, 262–271.
- [20] H. H. Kong, L. K. Wang, Q. Sun, C. Zhang, Q. G. Tan, W. Xu, *Angew. Chem. Int. Ed.* **2015**, *54*, 6526–6530; *Angew. Chem.* **2015**, *127*, 6626–6630.
- [21] H. H. Kong, L. K. Wang, Q. G. Tan, C. Zhang, Q. Sun, W. Xu, *Chem. Commun.* **2014**, *50*, 3242–3244.

Received: March 13, 2016

Revised: April 7, 2016

Published online: May 4, 2016